EARTH SCIENCES
RESEARCH JOURNAL

Earth Sci. Res. J. Vol. 25, No. 2 (June, 2021): 255-262

UNIVERSIDAD NACIONAL DE COLOMBIA

GEOLOGY

Application of artificial intelligence in lithology recognition of petroleum logging in low permeability reservoirs

Fuhua Shang[1], Maojun Cao[1*], Caizhi Wang[2]
[1]School of Computer & Information Technology, Northeast Petroleum University, Daqing, 163318, China
[2]Department of Well Logging & Remote Sensing Technology, Research Institute of Petroleum Exploration and Development, Beijing, 100083, China
*Corresponding author: caomj007@126.com

ABSTRACT

In low permeability reservoirs, the conversion accuracy of the existing petroleum logging lithology identification method to small pore capillary pressure curve is not high, resulting in a low rock mass identification accuracy. Therefore, artificial intelligence technology is considered in this study to enhance the accuracy of lithology identification in low permeability reservoirs. Firstly, the radar mapping program is used to predict the position of reservoir oil logging, and then the small pore capillary pressure curve is converted by using the conversion method of piecewise power function scale to obtain the pore characteristics of low-permeability reservoir rocks. On this basis, the crossplot method is used to gather the pore characteristic data in well logging and form a plan, and the response parameters of well logging rock mass are obtained to realize the identification and analysis of lithology. The experimental results show that, compared with the existing identification methods, the accuracy of lithology identification in low-permeability reservoir logging is significantly increased after the application of artificial intelligence technology, and the identification process takes less time, which fully proves that the application of artificial intelligence technology is conducive to improving the performance of lithology identification.

Keywords: Artificial intelligence; Low permeability reservoir; Petroleum logging; Lithology identification

Aplicación de la inteligencia artificial en reconocimiento litológico de extracción de petróleo en yacimientos de baja permeabilidad

RESUMEN

En los yacimientos de baja permeabilidad, la precisión de conversión del método de identificación de litología de extracción de petróleo existente a la curva de presión capilar de poros pequeños no es alta, lo que da como resultado una baja precisión de identificación del macizo rocoso. Por lo tanto, en este estudio se considera la tecnología de inteligencia artificial para mejorar la precisión de la identificación litológica en yacimientos de baja permeabilidad. En primer lugar, el programa de mapeo de radar se usa para predecir la posición del registro de petróleo del yacimiento, y luego la curva de presión capilar de poros pequeños se convierte utilizando el método de conversión de la escala de función de potencia por partes para obtener las características de los poros de las rocas del yacimiento de baja permeabilidad. Sobre esta base, se utiliza el método de parcelas cruzadas para recopilar los datos característicos de los poros en el registro de pozos y formar un plan, y se obtienen los parámetros de respuesta del macizo rocoso del registro de pozos para realizar la identificación y análisis de la litología. Los resultados experimentales muestran que, en comparación con los métodos de identificación existentes, la precisión de la identificación litológica en el registro de yacimientos de baja permeabilidad aumenta significativamente después de la aplicación de tecnología de inteligencia artificial, y el proceso de identificación lleva menos tiempo, lo que demuestra plenamente que la aplicación de la tecnología de inteligencia artificial es propicia para mejorar el rendimiento de la identificación litológica.

Palabras clave: Inteligencia artificial; Embalse de baja permeabilidad; Explotación de petróleo; Identificación de litología

Record
Manuscript received: 05/07/2019
Accepted for publication: 02/10/2019

How to cite item
Shang, F., Cao, M., & Wan, C. (2021). Application of artificial intelligence in lithology recognition of petroleum logging in low permeability reservoirs. *Earth Sciences Research Journal*, 25(2), 255-262. DOI: https://doi.org/10.15446/esrj.v25n2.80895

ISSN 1794-6190 e-ISSN 2339-3459
CC BY
https://doi.org/10.15446/esrj.v25n2.80895

Introduction

With the development and progress of the society, the demand for energy in various fields is constantly increasing. Therefore, petroleum geological exploration technology is facing more severe challenges. Multi - channel, multi - means, multi - discipline cross - fusion has become the development trend of exploration and development technology (Deng et al., 2017).

The early geological exploration objects in China are mainly sand and mudstone reservoirs, and lithology identification is relatively simple. With the continuous development of geological exploration and development, the requirement of well logging technology is gradually improved, and in order to form a more reasonable well logging interpretation method, lithology identification technology is also improved. Lithology identification belongs to the category of logging engineering and is an important research content in reservoir description, formation evaluation and drilling monitoring. The commonly used methods to obtain formation lithologic information include cuttings logging, coring section analysis and comprehensive treatment of logging data (Wei et al., 2017). Among them, the quality of cuttings logging depends on the operation of technicians, which is greatly influenced by human factors. The process of core slice analysis is time-consuming and laborious, and it is difficult to describe the complete well formation profile. In terms of comprehensive processing of logging data, crossplot method can intuitively reflect the boundary interface and lithological distribution area of different lithologies, and has the advantage of intuitive reading. However, its operation process is complex, and it cannot identify the whole well or interpret lithological information of the well. The mathematical statistical method is suitable for well logging data with good physical characteristics, and has a good application effect when there are few core data and more logging data, but it is very difficult to obtain the empirical formula (Xie et al., 2018; Jia et al., 2018; Jiang et al., 2018).

Artificial intelligence is a branch of computer science. It is a technology used to simulate, extend and expand human intelligence. It can simulate human consciousness, thinking and information formation process. Research in this field includes robotics, language recognition, image recognition, natural language processing and expert systems. It can be said that artificial intelligence is a very challenging science, which requires not only computer knowledge, but also knowledge in fields such as psychology and philosophy (Deng et al., 2018). Artificial intelligence research, on the whole, one of the main goal is to make the machine to be able to do some human intelligence is needed to complete a complex work, namely through the use of computers to simulate human thinking process and intelligent behavior of the discipline, can say it is almost covered all subjects of natural science and social science, its scope has been far beyond the scope of computer science (Guzman & Aoyama, 2018).

In recent years, artificial intelligence has become one of the main methods of pattern recognition in various fields. For example, BP neural network and fuzzy cluster analysis method. Although the BP neural network method has some disadvantages such as local minimization, slow convergence rate and different structure selection, it has the ability of distributed processing, self-learning, self-organization, highly nonlinear mapping and fault tolerance, which greatly makes up for the deficiency of self-recognition performance.

Therefore, in order to improve the ability of identifying lithology of oil logging in low permeability reservoirs, artificial intelligence technology is introduced in this study.

Application research on reservoir oil logging location prediction

When predicting the location of reservoir oil logging, first of all, do not collect logging data. In this process, various interference factors inevitably exist, which affect the resolution of the signal. Linear combination of sensitive indexes with high correlation is an effective method to improve the accuracy of logging interpretation. Therefore, on the basis of selecting the logging data of the core well, the logging data is compared with the core data by the multi-index radar chart comparison method. The execution flow of the radar chart drawing program is shown in Figure 1.

According to the implementation process of the radar chart drawing program as shown in Figure 1, sensitive indexes that can reflect the lithologic

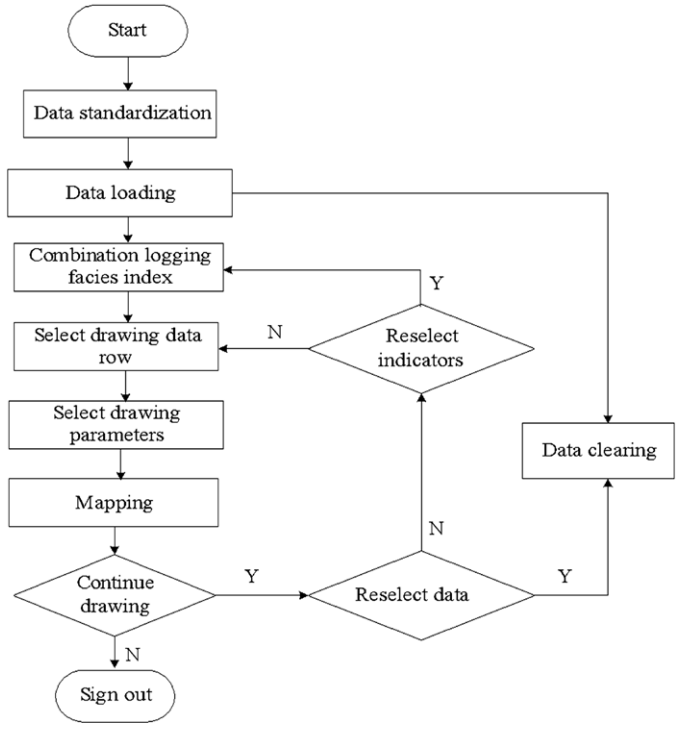

Figure 1. Radar chart drawing program execution flow diagram

change characteristics are selected, and then the correlation coefficient of the selected sensitive indexes is obtained, and the indexes with good correlation are combined linearly. Although the noise is random in the radar map drawing process, the linear combination process can enhance the formation characteristic information, and highlight the useful information by superposition signal, thus reducing the signal interference (Han et al., 2019).

The dimensions of different logging indicators are often different. In order to combine the indicators of different dimensions, it is necessary to normalize the indicators and then combine the dimensionless data to form new analysis indicators. Firstly, the radar map is used to analyze the logging data, and the log phase identification curve set is established through the standard well. Then, the logging location of the reservoir of the unknown well segment is identified by using the curve difference comparison, and the logging data of the core well is obtained after sorting out and correcting the analysis data, and the clustering normalization is completed. After calculation, the following results can be obtained:

$$X = \frac{x^* - x^*_{\min}}{x^*_{\max} x^*_{\min}} \tag{1}$$

Among them, X represents the normalized log curve, x^* represents the original log data, $x^*_{\min}$ and $x^*_{\max}$ represent the maximum and minimum values of the log curve respectively. It is easy to realize the linear normalization method with the powerful matrix operation of MATLAB, but in the transverse comparative analysis of multiple Wells, the difference of normalization results will be caused by the different selection of maximum and minimum values, thus affecting the analysis results. Therefore, data expansion or shift processing is carried out in this paper according to the value situation (Zhou et al., 2019; Jia & Deng, 2018). For example, after analyzing logging and core data, it can be seen that a certain reservoir is located in the second section, which is dominated by grayish-white medium-grain lithic sandstone, and its density (DEN) value is mostly around 2~3 g/cc. At this point, if we can extract the fractional part, magnify the difference between maximum and minimum, we will get a better comparison effect. On this basis, all the above density measurements were summarized and five parameters of AC, DEN, CNL, GR and RD were selected to depict the logging phase position radar map of the traveling gas layer, gas bearing layer and gas layer, as shown in Figure 2.

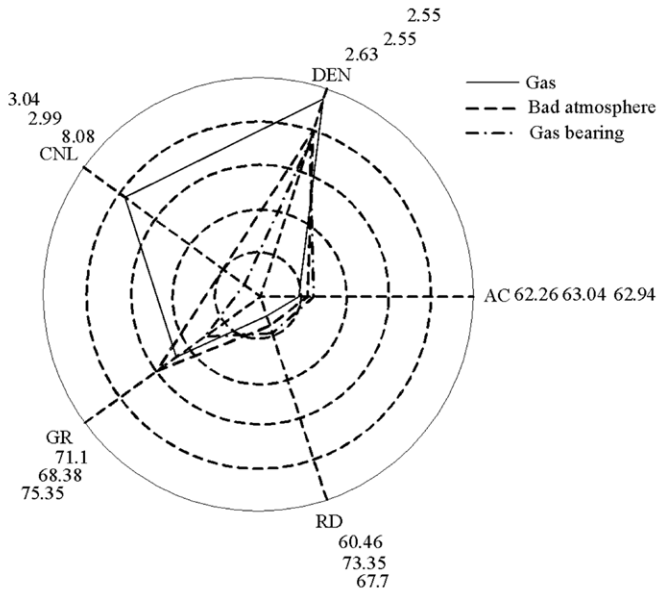

Figure 2. Logging locations corresponding to different density values

According to the different density ranges shown in Figure 2, it is obvious that CNL can reflect different density differences to a certain extent, which corresponds to the location of oil logging in low-permeability reservoirs. Samples of rock sections are randomly selected within the determined location range to determine the pore characteristics of rocks in low-permeability reservoirs.

Pore characteristics of low permeability reservoir rock

When judging non-uniform properties of low permeability reservoirs, pressure pump experiments should be carried out in low permeability reservoirs according to thin sections obtained by well logging, and rock characteristic data information should be obtained by nuclear magnetic test. The characteristic data are shown in Table 1.

Referring to the data information in Table 1, the "three porosity component percentage method" was used to process the above 26 rock samples, to qualitatively classify the pore types of the rock samples, and to draw the corresponding cross plot of pore structure parameters (Wang & Siau, 2019), as shown in Figure 3.

By referring to the cross plot of pore structure parameters shown in Figure 3, it can be seen that the T_2 spectrum measured by NMR consists of three kinds of transverse relaxation time, that is, the T_2 spectrum observed is:

$$\frac{1}{T_2}=\frac{1}{T_{2B}}+\frac{1}{T_{2D}}+\frac{1}{T_{2S}} \tag{2}$$

Table 1. Rock mass characteristic data table

Serial number of rock mass	Porosity/ %	T_2cutoff/ ms	NMR bound water saturation/ %	Maximum throat radius /μm	Mean throat radius/μm	Sorting coefficient	Expulsion pressure/ Mpa	T_2LM/ ms	Permeability/ 10^{-3}μm^{-2}
12-1	6.71	22.68	64.26	11.92	0.44	0.14	0. 26	1.70	0.07
61-1	6.77	21.99	65.77	11.41	0.60	0.16	0.31	1. 26	0.13
64-1	7.89	11.01	73.22	575	0.55	0.05	-0.31	1.36	0.11
62R	13.50	16.26	43.01	21.25	1.00	0.05	-0.43	0.75	0. 56
18.00	6.90	7.90	42.21	11.06	1.22	0.04	-0.66	0.61	0. 28
51B	10.60	18.00	40.60	26.24	1.15	0.12	-0.18	0.65	0.42
9-35	6.99	2.66	52.40	3.96	1.19	0.02	-0.94	0.63	0.68
70-1	5.62	1.55	57.21	1.93	0.33	0.00	-0.86	2.28	0.08
19-1	9.73	16.79	41.10	28.16	1.17	0.06	-0.31	0.64	0.23
34-4	12.77	5.85	46.97	9.78	2.60	0.21	-0.20	0.29	3.59
52-1	11.37	10.54	83.37	3.01	0.34	0.05	-0.42	2.21	0.15
64-1	8.12	7.41	64.15	6.47	0.89	0.07	-0.46	0. 84	0.41
93-1	16.65	8. 26	42.68	17.19	20.06	0.17	-0.53	0. 20	42.30
115-1	14.92	10.39	52.38	10.46	3.81	0.03	-0.74	0.56	4. 85
9-1	11.57	6. 80	61.11	5.54	1.35	0.07	-0.32	0.17	0.91
20-1	11.76	6.67	46.52	9.32	4.29	0.91	0.41	0.98	17.27
68-1	6.38	2.75	85.97	1.09	0.76	0.02	-0. 94	1.39	157
137.00	10.45	7.77	79.32	2. 98	0.54	0.03	-0.75	1.40	0.79
152-1	8.35	40.30	83.07	7.01	0.54	0.04	-0.48	0.98	0.87
3-1	6.26	27.35	67.35	9.17	0.76	0.30	0.81	2.01	0.63
30-1	5.52	1.68	91.38	0. 87	0.37	0.04	-0.40	0.22	0.52
91-1	10.56	13.81	45.54	15.45	3.35	0.19	-0.20	1. 26	3.38
144-1	8.21	61.52	67.08	35.12	0.60	0.10	-0.02	1.09	0.70
216-1	9.47	52.66	59.96	41.56	0.69	0.17	0.23	1.23	0.97
236-1	8.17	36.92	62.34	27.80	0.61	0.16	0.34	1. 20	0.85
257-1	6.90	46.74	56.18	42.06	0.63	0.21	0.62	0. 20	0.42

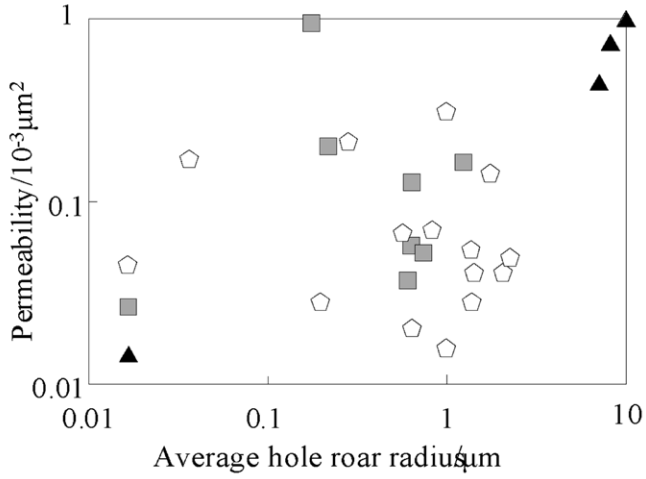

Figure 3. Cross plot of pore structure parameters

Where, T_2 denotes transverse relaxation time, T_{2B} denotes volumetric (free) relaxation time of the fluid, T_{2D} denotes diffusive relaxation time, and denotes surface relaxation time. T_{2S} and T_{2D} were characterized by specific surface area, diffusion coefficient, magnetic field gradient, echo interval and other parameters, and then:

$$\frac{1}{T_2}'=\frac{1}{T_{2B}}+\rho_2\left(\frac{S}{V}\right)+\frac{D(\gamma GT_E)^2}{12} \tag{3}$$

Among them, ρ_2 represents the transverse surface relaxation strength of the rock, S represents the surface area of pores, V represents the volume of pores, V represents the specific surface area of characterized rock samples, D represents the diffusion coefficient, G represents the magnetic field strength, T_E represents the echo interval, γ represents the magnetic rotation ratio, and the remaining parameters remain unchanged. For the uniform magnetic field with a small echo interval, Equation (2) can be transformed into:

$$\rho_2\left(\frac{\mathrm{S}}{\mathrm{V}}\right)=\frac{1}{\mathrm{T}_2}'=F_S\frac{\rho_2}{R_c} \tag{4}$$

Where, F_S represents the geometric shape factor, and for spherical pores, the value of F_S is 3; For columnar pores, F_S has a value of 2. R_C represents the pore radius.

Generally speaking, the relaxation time of pore fluid is related to the size and shape of pore space (Grzonka et al., 2018; Gobashy et al., 2020). Since there should be a corresponding transverse relaxation time for a particular R_C, T_2 and R_C should have a one-to-one correspondence. However, due to the constant change of F_S, the corresponding relationship between T_2 and R_C also changes. For medium - high porosity and permeability reservoirs, reservoir heterogeneity is weak, and the corresponding relationship between T_2 and R_C has little change. However, for tight sandstone reservoirs with complex pore structure and pore type, the corresponding relationship between T_2 and R_C changes greatly due to their strong reservoir heterogeneity.

According to fluid mechanics, there is a certain relationship between capillary pressure and pore radius:

$$P_c=\frac{2\sigma\cos\theta}{R_c} \tag{5}$$

Where, P_c represents capillary pressure, σ represents fluid interfacial tension, and θ represents wetting contact Angle. For mercury-air system, Equation (4) can be rewritten as:

$$P_c'=\frac{0.735}{R_c} \tag{6}$$

The comprehensive calculation formulas (3) and (5) can be obtained as follows:

$$C=P_c\times\mathrm{T}_2 \tag{7}$$

Where, C represents the conversion coefficient, and. Therefore, if the conversion coefficient can be accurately calculated by using the well log, the capillary pressure curve at different depths of the whole well can be evaluated by using the NMR log, and the variation of various pore structure parameters with depth can also be evaluated (Zibret, 2019).

Generally, the pseudo-capillary pressure curve and the capillary pressure curve of the pore segment cannot be superimposed together, because of the accumulation of thin film bound water with large pores in T_2 distribution to small pores (Zhang, 2019). Based on this idea, a piecewise power function calibration method is proposed to solve the problem of low precision of pressure curve conversion of small pore capillary. In theory, the specific surface area has a linear relationship with the pore size, but for the actual formation, the pore structure is very complex, and the specific surface and pore size often have a nonlinear relationship, which can be expressed as follows:

$$f(R_c)=\frac{\rho_2}{\frac{1}{\mathrm{T}_2}} \tag{8}$$

Where, $f(R_C)$ represents the function of R_C. According to Equation (5) and Equation (7), the function of T_2 spectrum can be calculated as follows:

$$g\left(\frac{1}{\mathrm{T}_2}\right)=P_c \tag{9}$$

According to the above formula, the pore characteristics of low-permeability reservoir rocks can be divided into large pores and small pores, and the pore characteristics can be described as follows:

$$\begin{cases}P_{cb}=a_1\left(\dfrac{1}{\mathrm{T}_2}\right)^{b_1}\\ P_{cs}=a_2\left(\dfrac{1}{\mathrm{T}_2}\right)^{b2}\end{cases} \tag{10}$$

Where, a_1 and b_1 represent the corresponding parameters of small pores, and a_2 and b_2 represent the corresponding parameters of large pores. Referring to the pore characteristics obtained, crossplot method can be used to obtain logging response characteristics that can represent lithology.

Obtain logging rock mass response parameters

The cross-plot method is used to summarize the pore data obtained above and form a plan. According to the coordinates of the intersection point, the numerical value and aggregation trend of the parameters can be seen. In the process of using the crossplot method to identify lithology, two groups of appropriate logging data are first selected, and coordinate points are drawn in the crossplot coordinate system according to the changes of logging data. The aggregation trend of coordinate points is expressed in the form of intuitive data, and the distribution range and boundary of different lithology can be reflected visually. The crossplot drawn should be compared with the coring lithology data for better accuracy of lithology identification. Cross-graphs such as GR-PB and GR-AC can be made according to the core analysis data. According to these cross-graphs, the positions of different measured lithologic points, the lower limit of lithologic logging parameters and the lithologic distribution trend can be determined. Referring to logging rock masses of different densities and using the ratio of spectral intensity of elements, structural logging rock characteristic parameters are as follows:

$$Z = \frac{\phi^{0.5421} \times \overline{R}^{1.0458}}{S_p^{0.3181}} \tag{11}$$

Among them, Z represents logging rock characteristic parameters, ϕ represents porosity calculated above, R represents average pore throat radius, S_p represents sorting coefficient, and two constants represent permeability measured. Logging rock characteristic parameters were defined to be around 80-110, and the acoustic wave presented high value, which was generally above 67, with the development of porosity structure. When the characteristic parameters of logging rocks are above 120 and the acoustic values are generally above 70, the fused tuff appears in the logging interior. When the characteristic parameters of logging rocks are distributed around 40-120 and the acoustic values are generally below 65, the characteristic values cannot be determined, and the rock mass is also a fused tuff. According to the calculated logging rock characteristic parameters, the cross map of Gr-ρb within the logging location was obtained, as shown in Figure 4.

As can be seen from the logging characteristic parameters shown in Figure 4, different rock assemblages have great differences in layers, and their electrical properties are also different. Therefore, before obtaining the response characteristics in the logging, linear transformation should be adopted to normalize the electrical properties in the logging characteristic parameters, and the standardization process is as follows:

$$\begin{cases} x_{T_i}^n = \dfrac{x_i^n - \overline{x_i}}{\sigma_i} \\ \overline{x_i} = \dfrac{1}{N}\sum_{n=1}^{N} x_i^n \\ \sigma_i = \sqrt{\dfrac{1}{N-1}\sum_{n=1}^{N}(x_i^n - \overline{x_i})^2} \end{cases} \tag{12}$$

Where, Where, 111 represents the n the standardized value of x_i, $\overline{x_i}$ represents the mean value of the electrical variable, σ_i represents the standard deviation of the electrical variable, and N represents the number of logging characteristic parameters. The response values of acoustic time difference (AC), natural gamma (GR) and resistivity (RT) obtained by using the above standardized electrical property values combined with the curve overlap method are comprehensively judged. The difference, acoustic time difference (AC), natural gamma (GR) and resistivity (RT) of porosity ϕ_D and ϕ_N extracted by the overlapping method are shown in Table 2.

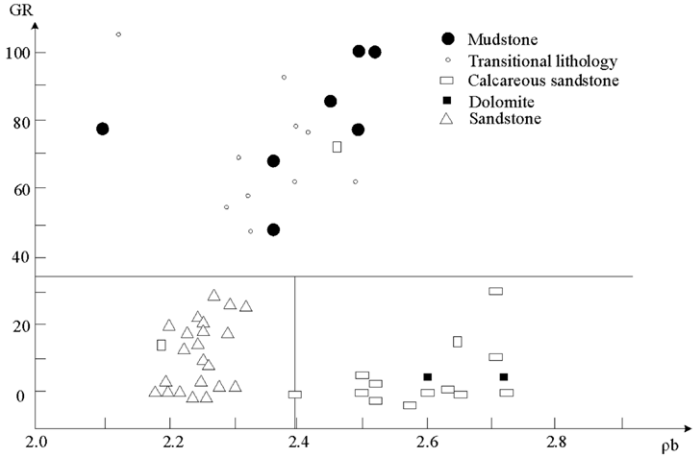

Figure 4. Gr-ρb cross map of oil logging in low permeability reservoir

Table 2. Parameter set matrix table

Overlapping layer	$\phi_D - \phi_N$	The mean AC(us/ft)	The mean GR(API)	The mean RT(Ω·m)
1	-0.179	53.094	49.902	230.441
2	-0.143	53. 512	54.729	235.899
3	-0.135	53. 539	52.784	238.887
4	-0.132	53. 539	47.642	242.040
5	-0.089	52. 870	42.829	253.606
6	-0.011	51.491	39.953	263.617
7	-0.056	50.794	41.874	268.003
8	-0.081	50.525	45.082	285.795
9	-0.105	50.318	47.851	321.116
10	-0.108	50.347	45.627	337.462
11	-0.110	50.453	45.927	339.846
12	-0.109	50.542	43.827	294.277
13	-0.121	50.374	42.100	263.586
14	-0.085	53.412	49.902	213.427

The data shown in Table 2 are integrated into the calculation formula of logging response characteristic parameters, as shown below:

$$\begin{cases} N = \dfrac{\phi_{nf} - \phi_{Nma}}{\rho_{ma} - \rho_f} \\ M = \dfrac{\Delta t_f - \Delta t_{ma}}{\rho_{ma} - \rho_f} \end{cases} \tag{13}$$

Among them, Δt_f represents acoustic time difference of pore fluid, Δt_{ma} represents acoustic time difference of rock skeleton, ρ_{ma} represents pore fluid density, ϕ_{ma} represents neutron porosity of rock skeleton, and ϕ_{nf} represents neutron porosity of pore fluid. By referring to the calculation results of different characteristic parameters, the response values of corresponding logging lithology were calculated, as shown in Table 3.

Table 3. Response values of logging lithology

Logging lithology	AC (us/ft)	DEN (g/cm³)	CNL (p.u.)	GR (API)
Cloud mass limestone	45.25~47	2.17~2.79	-1~0	10
Gray dolomite	43.5~45.25	2.79~2.81	0~1	10
Limestone	48	2.71	-1	10
Dolomite	43.50	2.87	1	10
Argillaceous Limestone	59	2.12	21.50	57.50
Anhydrite	49.30~51.80	2.91~3.02	-2	1.50~6
Paste dolomite	43.50~46.75	2.87~2.91	-1~0.50	5.80~10
Cream quality Limestone	49	2.71~2.915	-1.50~1	5.80~10

Corresponding to the response values of different characteristics shown in Table 3, the properties of different logging rocks can be determined. Thus, the application of artificial intelligence in lithology identification of low permeability reservoirs is completed.

Simulation experiment and result analysis

In order to verify the practical application performance of the low permeability reservoir logging lithology identification method designed in this paper by using artificial intelligence, the following simulation experiment is designed for verification.

The experiment to prepare

Firstly, a basic LIBS detection system is set up, which mainly includes light source, light splitting system, photoelectric detector, timing control module, collimation, focusing light path, light collection lens group, sample table and so on. Imaging of laser-induced plasma is also required during the experiment, so imaging modules should be set up in the LIBS detection system. The experimental platform structure is shown in Figure 5.

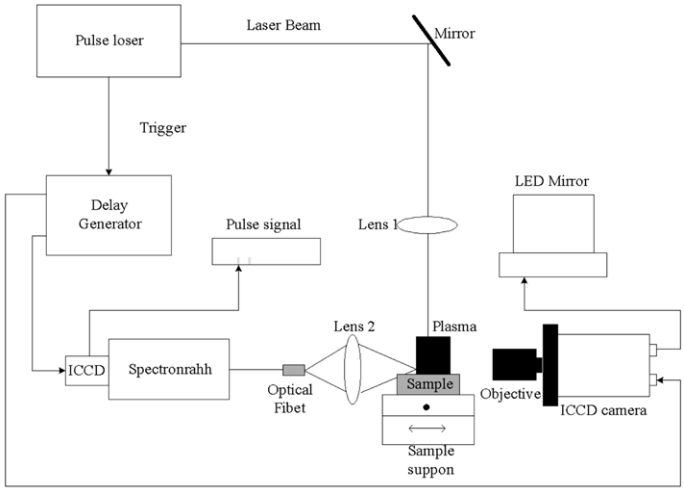

Figure 5. Experimental platform structure diagram

As shown in Figure 5, the main performance parameters of the ME5000 medium-step grating spectrometer in the experimental platform are shown in Table 4.

Table 4. Main performance parameters of ME5000 medium - step grating spectrometer

Parameter		Data
Escher spectrometer	Focal length (mm)	195
	Aperture	F7
	Wavelength range (nm)	230~950
	Wavelength accuracy (nm)	±0.05
	Focal plane size (mm)	13.3×13.3
	Stray light	1.5×10^{-4}
ICCD	Active pixel	1024×1024
	Effective pixel size (Nm)	13
	Effective area (mm)	13.3×13.3
	Peak quantum efficiency	up to 18%
	Total insertion delay (NS)	~35
DDG	Insert delay (NS)	~19
	Gate delay	0~25s
	Delayed resolution	25ps
	Width of the gate	1ns~25s
	Width resolution	25ps

Under the control of the performance parameters shown in Table 4, 8 logging blocks as shown in Figure 6 are prepared.

Use as shown in Figure 6 to mudstone, shale, sandstone, dolomite, asphalt, volcanic ash, conglomerate and paste rock, in the experimental environment, were used in this paper, design of using artificial intelligence low permeability oil reservoir logging lithology identification method and the traditional lithology recognition method based on laser induced breakdown spectroscopy, logging lithology recognition method based on Boosting Tree algorithm comparing experiment, from lithology recognition accuracy and recognition process takes two Angle compared three methods of recognition performance.

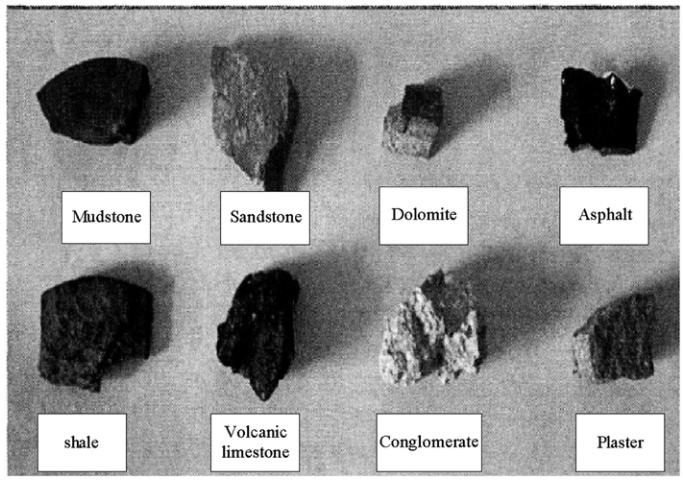

Figure 6. Experiment to prepare rock samples

Experimental results and analysis

Taking mudstone samples as an example, based on the above experimental preparation, the standard reference spectrum of mudstone samples was first obtained by using ME5000 medium-step grating spectrometer, as shown in Figure 7.

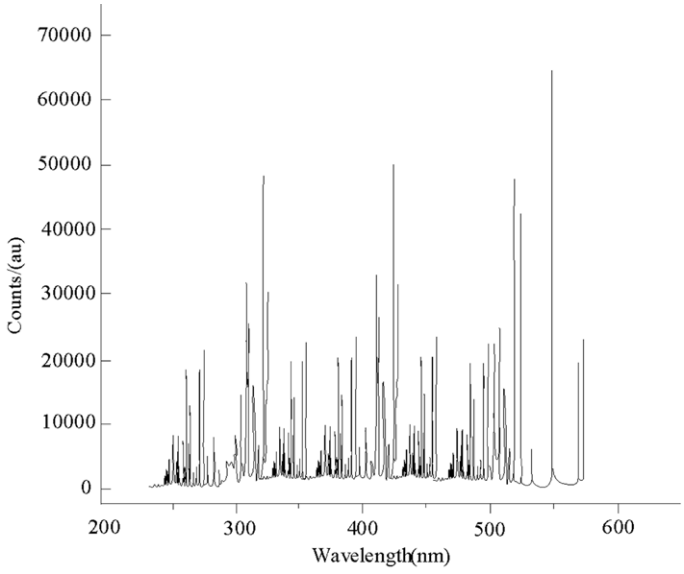

Figure 7. Standard reference spectra of mudstone samples

After obtaining the standard spectrum of mudstone samples, under the same experimental conditions, used respectively in this paper, the design of the use of artificial intelligence in the low permeability oil reservoir logging lithological identification method and the traditional lithology recognition method based on laser induced breakdown spectroscopy, logging lithology recognition method based on Boosting Tree algorithm for mudstone samples of spectral information. In order to avoid the spectral line position drift caused by temperature change, the experimental room temperature should be controlled within the range of 25-30 °C. On this basis, the similarity between the spectral information of mudstone samples obtained by three different identification methods and the standard spectra was compared. When the position and relative strength of spectral lines between the three different identification methods were consistent, the recognition was deemed as a success. The recognition results obtained by the three recognition methods are shown in Table 5.

According to the experimental results shown in Table 5, the three identification methods can be used to identify the same number of different types of logging rock mass information, and the three identification methods

Table 5. Statistical table of identification results of different methods

Rock mass classification	Number of test samples /number	Logging lithology identification method based on Boosting Tree algorithm		Method of this paper		Lithology identification method based on laser induced breakdown spectroscopy	
		Correctly identify quantity/number	Recognition accuracy/%	Correctly identify quantity/number	Recognition accuracy/%	Correctly identify quantity/number	Recognition accuracy/%
Mudstone	8	4	50	8	100	6	75
Sandstone	8	3	37.5	8	100	5	62.5
Shale	8	4	50	7	87.5	6	75
Volcanic ash	8	3	37.5	8	100	7	87.5
Dolomite	7	3	42.8	6	85.7	5	71.4
Cream rock	2	1	50	2	100	2	100
Conglomerate	7	5	71.4	7	100	6	85.7
Asphalt	4	2	50	4	100	3	75

show different identification capabilities. After applying the logging lithology identification method based Boosting Tree algorithm, the number of rock masses identified is too small and the identification accuracy is low. However, the identification accuracy of lithology based on laser-induced breakdown spectroscopy has been improved, but the information of other rock masses has not been fully identified except for the gypsum rock. After the application of this method, except dolomite and shale, the information of other rock mass is correctly identified, and the correct identification rate of this method is the largest among the three methods. Based on the above experimental results, it can be seen that the rock mass identification method designed in this paper with artificial intelligence technology can avoid the deficiency of identifying too few rock masses, and the identification accuracy is higher, which is suitable for the identification of lithology of oil logging in low-permeability reservoirs.

On this basis, the identification performance of the three methods is verified by taking the identification process time as the index. The results are shown in Figure 8.

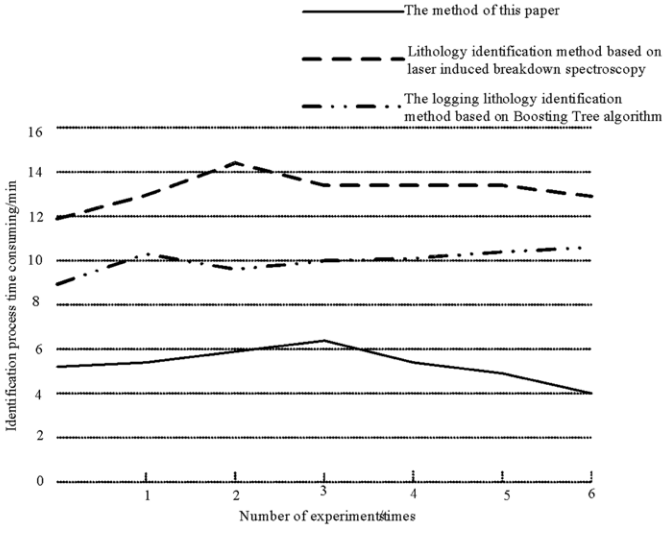

Figure 8. Time - consuming comparison diagram of different methods to identify the process

According to the experimental results shown in Figure 8, the three identification methods can be used to identify the same number of different types of logging rock mass information, and the time of the three identification methods is greatly different. The well logging lithology identification method based on Boosting Tree algorithm has a identification process of 8-12min. The lithology identification method based on laser induced breakdown spectroscopy technology is higher and keeps between 12-15min. However, the identification process of the method in this paper takes the least time among the three methods, which is always kept below 7min. Based on the above experimental results, it can be seen that the rock mass identification method designed in this paper with artificial intelligence technology can quickly identify the lithologic characteristics of oil logging in low-permeability reservoirs.

Conclusion

Automatic identification of lithology is based on the combination of mathematical theory and computer software. This process fully embodies the interdisciplinary application, which can be used as a supplement to the conventional lithology identification method and promote the development of the lithology identification technology with multiple approaches, methods and angles. The appearance of artificial intelligence lithology identification software plays a powerful role in promoting the technology of complex formation lithology classification. In this paper, the application of artificial intelligence technology to low permeability reservoir oil logging lithology identification is proposed. It has been proved by practice that this method can effectively improve the accuracy of lithology identification in low permeability reservoir, and the identification process is time-consuming.

Acknowledgments

This paper is supported by National Science and Technology Major Project "Well Logging Interactive Fine Fusion Processing Platform" (No. 2017ZX05019-005), Heilongjiang Natural Science Foundation "Quantum Intelligent Optimization and Application in Real-time Adjustment of Logging Interpretation Model While Drilling" (No. LH2019f004).

Reference

Deng, L. (2018). Artificial intelligence in the rising wave of deep learning: the historical path and future outlook [perspectives]. IEEE Signal Processing Magazine, 35(1), 180-177. DOI: 10.1109/MSP.2017.2762725

Deng, C. X., Pan, H. P., & Luo, M. (2017). Joint inversion of geochemical data and geophysical logs for lithology identification in CCSD Main Hole. *Pure and Applied Geophysics*, 174(12), 4407-4420. https://doi.org/10.1007/s00024-017-1650-7

Gobashy, M., Abdelazeem, M., Abdrabou, M., & Khalil, M. H. (2020). Estimating model parameters from self-potential anomaly of 2D Inclined sheet using whale optimization algorithm: applications to mineral exploration and tracing shear zones. *Natural Resources Research*, 29 (1), 499-519. https://doi.org/10.1007/s11053-019-09526-0

Grzonka, D., Jakóbik, A., Koodziej, J., & Pllana, S. (2018). Using a multi-agent system and artificial intelligence for monitoring and improving the cloud performance and security. *Future generation computer systems*, 86(SEP.), 1106-1117. DOI:10.1016/j.future.2017.05.046

Guzman, A., & Aoyama, A. (2018). Pipeline risk assessment using artificial intelligence: a case from the Colombian oil network. *Process Safety Progress*, 37(1), 110-116. DOI:10.1002/prs.11890

Han, F. L., Zhang, H. B., Guo, Q., & Rui, J. (2019). Lithological identification with probabilistic distribution by the modified compositional Kriging. *Arabian Journal of Geosciences*, 12(18), 1-14. DOI:10.1007/s12517-019-4775-4.

Jia, H., & Deng, L. H. (2018). Water flooding flowing area identification for oil reservoirs based on the method of streamline clustering artificial intelligence. *Petroleum Exploration and Development*, 45(02), 328-335. https://doi.org/10.1016/S1876-3804(18)30036-3

Jia, J. W., Fu, H. B., & Wang, H. D. (2018). Lithology identification methods based on laser-induced breakdown spectroscopy technology. *Chinese Journal of Quantum Electronics*, 35(03), 264-270.

Jiang, K., Wang, S. D., & Hu, Y. J. (2018). Lithology identification model by well logging based on boosting tree algorithm. *Well Logging Technology*, 42(04), 395-400.

Wang, W. Y., & Siau, K. (2019). Artificial intelligence, machine learning, automation, robotics, future of work and future of humanity: a review and research agenda. *Journal of Database Management*, 30(1), 61-79. DOI:10.4018/JDM.2019010104

Wei, J. L., Liu, X. N., Ding, C., Liu, M., Jin, M., & Li, D. (2017). Developing a thermal characteristic index for lithology identification using thermal infrared remote sensing data. *Advances in space research*, 59(1), 74-87. https://doi.org/10.1016/j.asr.2016.09.005

Xie, Y. X., Zhu, C. Y., Zhou, W., Li, Z., Liu, X., & Tu, M. (2018). Evaluation of machine learning methods for formation lithology identification: A comparison of tuning processes and model performances. *Journal of Petroleum Science and Engineering*, 16(03), 182-193. https://doi.org/10.1016/j.petrol.2017.10.028

Zhang, L., Liang, Y. C., & Niyato, D. (2019). 6g visions: mobile ultra-broadband, super internet-of-things, and artificial intelligence. *China Communications*, 16(8), 1-14. DOI: 10.23919/JCC.2019.08.001

Zhou, Y., Zhang G. Z., Gao G., Zhao, W., Yi, Y., & Wei, H. (2019). Application of kernel principal component analysis in lithologic identification of well logging turbidite. *Oil Geophysical Prospecting*, 54(03), 667-675, 490.

Zibret, G. (2019). Influences of coal mines, metallurgical plants, urbanization and lithology on the elemental composition of street dust. *Environmental Geochemistry and Health*, 41(3), 1489-1505. DOI: 10.1007/s10653-018-0228-3